

The distinct roles of Argonaute protein 2 in the growth, stress responses and pathogenicity of the apple tree canker pathogen

H. Feng¹ | M. Xu¹ | Y. Liu¹ | X. Gao¹ | Z. Yin¹ | R. T. Voegelé² | L. Huang¹ 

¹College of Plant Protection and State Key Laboratory of Crop Stress Biology for Arid Areas, Northwest A&F University, Yangling, China

²Institut für Phytomedizin, Universität Hohenheim, Stuttgart, Germany

Correspondence

Lili Huang, College of Plant Protection and State Key Laboratory of Crop Stress Biology for Arid Areas, Northwest A&F University, Yangling, China.
Email: huanglili@nwsuaf.edu.cn

Funding information

National Natural Science Foundation of China, Grant/Award Number: 31501591; China Postdoctoral Science Foundation Special Funding, Grant/Award Number: 2016T90953; Doctoral Scientific Research Foundation of Northwest A&F University

Editor: S. Woodward

Summary

Valsa mali (*V. mali*), the causal agent of apple tree *Valsa* canker, severely damages apple production, a major economic crop in China. To date, our understanding of the molecular mechanisms associated with the pathogenicity of *V. mali* is still limited. RNA interference participates in various biological processes in multicellular organisms. The Argonaute proteins (AGOs), which are a core component of the RNA interference system, play key roles in vegetable growth, environmental responses and fungal pathogenicity. Previously, transcriptome analysis revealed that the AGO2 gene (*VMAGO2*) was up-regulated during *V. mali* infection, suggesting that *VMAGO2* plays a potential role in pathogenicity. In this study, we investigated the potential roles of *VMAGO2* in the growth, stress responses and pathogenicity of *V. mali*. *VMAGO2* was isolated and found to be orthologous to AGO2 of *Neurospora crassa* and *Fusarium graminearum*. Real-time quantitative PCR analysis showed that *VMAGO2* expression was 3.4-fold higher than that of the control (mycelium) at 24 hr post-inoculation (hpi). Six positive *VMAGO2* mutants were generated using double-joint PCR and PEG-mediated transformation. Deletion of *VMAGO2* did not result in any obvious phenotypic change when compared with that of wild-type strain 03-8. Furthermore, the colonial morphology was not obviously affected when the mutants were subjected to osmotic and pH stress treatments. However, the knockout mutants did not grow on PDA with 0.05% H₂O₂. More importantly, infection assays showed that the average lesion diameter/length resulting from mutant infections was 34.8% and 19.8% smaller on apple leaves and twigs, respectively, than those resulting from wild-type infections. All six positive mutants showed a consistent phenotype, and the defects of the mutants were fully complemented by re-introducing the WT *VMAGO2* allele. Our results demonstrated that *VMAGO2* plays an important role in H₂O₂ tolerance and the pathogenicity of *V. mali*.

1 | INTRODUCTION

Apple tree *Valsa* canker, which is caused by *Valsa mali*, a weak parasitic pathogen, is severely restricting the development of the apple industry in China (Cao, Guo, Li, Sun, & Chen, 2009; Wang, Zang, Yin, Kang, & Huang, 2014). Investigating the pathogenesis of *V. mali* is important for developing a resistance breeding strategy and for identifying new fungicide target sites; however, the molecular mechanisms underlying the

pathogenesis of *V. mali* are complex and not fully understood. Although recent analyses of the *V. mali* genome and transcriptome information have provided a means to explore the pathogenesis, and some pathogenesis-related genes have been identified and characterized (Ke et al., 2014; Li et al., 2015; Yin, Zhu, Feng, & Huang, 2016; Yin et al., 2015), the RNA interference (RNAi) pathway of *V. mali* is still unknown.

RNAi, which is mediated by small regulatory RNAs and a family of ribonucleo-protein complexes or RNA-induced silencing complexes

(RISCs), is a powerful mechanism of gene silencing that underlies many aspects of eukaryotic biology (Pratt & MacRae, 2009). There are several RNA processing pathways that can lead to the generation of various small RNAs (sRNAs), such as short interfering RNAs (siRNAs), microRNAs (miRNAs), transfer RNA-derived fragments (tRFs) and qiRNA (Agrawal et al., 2003; Bartel, 2004; Jöchl et al., 2008; Lee et al., 2009). These sRNAs can only guide gene silencing when they are bound to Argonaute proteins (AGOs) through a similar base-pairing mechanism with their target RNA transcripts (Kim, Heo, & Kim, 2010). Therefore, studying the functions of AGOs may lead to insights into potential new roles of RNAi.

As the core components of RISC, AGO proteins contain four domains: the N-terminal, PAZ, MID and PIWI functional domains. The PAZ and PIWI domains are the two main structural features of the AGO proteins (Joshua-Tor, 2004). The main function of the PAZ domain is to identify and combine with the two overhanging nucleotides at the 3' end of the small double-stranded RNA, while the function of the PIWI domain is to process mRNAs as it contains a catalytic centre (Jinek & Doudna, 2009; Yuan et al., 2005).

Argonaute proteins have been shown to play significant roles in regulating gene expression, chromosome structure and function, and virus defence mechanisms (Hutvagner & Simard, 2008). In *Drosophila*, AGO1 and AGO2 can participate in the generation of miRNAs and siRNAs, respectively (Okamura, Ishizuka, & Siomi, 2004). In plants, many AGOs have been reported to be involved in resistance to different pathogens (Agorio & Vera, 2007; Duan, Fang, & Zhou, 2012; Ellendorff, Fradin, de Jonge, & Thomma, 2009; Mallory & Vaucheret, 2010). AGO proteins have been highly conserved throughout evolution and are frequently present in eukaryotes. Similarly, AGO proteins are also present in the vast majority of filamentous fungi (Hu, Stenlid, Elfstrand, & Olson, 2013; Nunes, Sailsbery, & Dean, 2011). Previously, the function of AGOs in fungi has been primarily assessed based on phenotypic changes and changes in the sRNA levels in the AGO-knockout strains. In a model fungal system such as *Neurospora crassa*, *qde-2* (quelling deficient-2) and *SMS-2* (suppressor of meiotic silencing-2) are known to be involved in silencing meiosis, and *qde-2* is also associated with the generation of qiRNAs and miRNAs (Lee, Pratt, McLaughlin, & Aramayo, 2003; Lee et al., 2009). Among the four AGOs in *Cryphonectria parasitica*, only AGO2 is involved in inducing RNA silencing-mediated antiviral defence and promoting viral RNA recombination (Sun, Choi, & Nuss, 2009). Finally, nutritional stress-induced vegetative development and autolysis were significantly affected when the *ago-1* gene was deleted in *Mucor circinelloides*, indicating that *ago-1* may play a role in the response to environmental signals (Cervantes et al., 2013).

Based on the published genome sequence of *V. mali*, three AGOs (VMAGO1, VMAGO2 and VMAGO3) appeared to be present in this fungus (Yin et al., 2015). Interestingly, transcriptome analysis revealed that VMAGO2 was highly induced during *V. mali* infection (Ke et al., 2014), suggesting a potential regulatory role in the pathogen infection process. On the basis of this finding, this study was designed to further investigate the potential roles of VMAGO2 in the growth, stress

responses and pathogenicity of *V. mali*. The objective of this study was to provide insights into the potential mechanisms of sRNA-mediated regulation of *V. mali* infection.

2 | MATERIALS AND METHODS

2.1 | Fungal strains and vector

The wild-type strain 03-8 (WT) of *V. mali* was provided by the Laboratory of Integrated Management of Plant Diseases, College of Plant Protection, Northwest A&F University, Yangling, Shaanxi, PR China. Strains were maintained on potato dextrose agar (PDA) medium at 25°C in the dark. For DNA extraction, the strains were grown in liquid potato dextrose broth (PDB) medium. The fungal genomic DNA was extracted using the CTAB method (Möller, Bahnweg, Sandermann, & Geiger, 1992). The vector pBIG2RHPH2-GFP-GUS was used for gene deletion.

2.2 | Characterization of the VMAGO2 sequence

The VMAGO2 gene sequence was identified from the available *V. mali* genome database. The VMAGO2 gene sequences were deposited in GenBank under accession number KT191022. The domain architecture was analysed using InterProScan (<http://www.ebi.ac.uk/cgi-bin/iprscan/>). A phylogenetic analysis of the deduced protein sequence and the corresponding sequences of other species was performed using the DNAMAN, version 6.0.

2.3 | Generation of Δ VMAGO2 mutants

The double-joint PCR approach was used for vector construction to generate VMAGO2 deletion mutants (Yu et al., 2004). The strategy consisted of replacing VMAGO2 with the hygromycin-phosphotransferase (*hph*) cassette, which was amplified from PHIG2RHPH2-GFP-GUS using primers of HYG-F and HYG-R (Table S1). The upstream and downstream flanking sequences were amplified with primers of VMAGO2-1F/2R and VMAGO2-3F/4R, respectively (Table S1). The amplified fragments (upstream flanking sequence, *hph* and downstream flanking sequence) were fused using double-joint PCR (Yu et al., 2004). PCR production, amplified with the nested primer pair VMAGO2-CF/CR using the linear *hph* cassette as template, was concentrated and transformed to the protoplasm of the WT strain using the PEG-mediated transformation method described by Gao, Li, Ke, Kang, and Huang (2011). A single hypha from a colony of each transformant was placed in the centre of a PDA medium plate using the single hypha separation method. After culturing for 3 days in the dark at 25°C, the strains were transferred to PDA medium plates containing 50 µg/ml of hygromycin and 100 µg/ml of cephalosporin for three generations of continuous culture to positively select for hygromycin-resistant transformants. Hygromycin-resistant transformants were screened by PCR using the VMAGO2-5F/6R and H852/H850 primers, and confirmed using the VMAGO2-1F/H855R and H856F/VMAGO2-4R primers (Table S1, Figure S1). Putative mutants

were further confirmed by Southern blot analysis. The genomic DNA of WT and $\Delta VMAGO2$ mutants was isolated and digested using the *Xho I* and *Pst I* restriction enzymes. The *HYG* probe was amplified with the H850/H852 primers, and the *VMAGO2* probe was amplified with the *VMAGO2*-5F/6R primers. The detailed procedure for Southern blot was followed to the manufacturer's instructions of the DIG DNA Labeling and Detection Kit II (Roche, Mannheim, Germany).

2.4 | Observations of the colonial morphology of mutants and WT strains

Mycelial agar discs (5-mm-diameter) of the $\Delta VMAGO2$ and $\Delta VMAGO2$ -C mutant strains and the WT strain were placed in the centre of PDA medium plates and cultured in the dark at 25°C. All the studies were conducted in triplicate with three Petri dishes in each repetition. The colonial morphology was photographed after 2 days of incubation.

2.5 | Measurement of stress responses

To determine the sensitivity of the strains to osmotic stress, 5-mm-diameter mycelial agar discs of the $\Delta VMAGO2$ and $\Delta VMAGO2$ -C mutant strains and the WT strain were placed on PDA plates containing different concentrations of NaCl (0.1, 0.5 or 1.0 M) or KCl (0.5, 1.0 or 1.5 M). After 7 days of incubation, the morphology of the colonies was examined and photographed. To determine the sensitivity of the mutants and WT to different pH levels, the colonies were grown on PDA plates with different pH values (pH 2–11) at 25°C in the dark. After 2 days of incubation, the colonies were photographed and the diameters of the colonies were measured. To determine the sensitivity of the strains to oxygen radicals, 5-mm-diameter mycelial agar discs of the $\Delta VMAGO2$ and $\Delta VMAGO2$ -C mutant strains and the WT strain were placed on PDA plates containing 0.05% H₂O₂ and cultured in the dark at 25°C. The diameters and morphologies of the colonies were examined on the third and seventh day. All the studies were conducted in triplicate, with three Petri dishes in each repetition. The statistical significance was determined using the protected Fisher's least significant difference (LSD) test ($p < .05$) or the Student's *t* test ($p < .05$) using SPSS18 software.

2.6 | Pathogenicity test

"Fuji" apple (*Malus domestica* Borkh. cv "Fuji") leaves and twigs were used for assaying the pathogenicity of the $\Delta VMAGO2$ mutants. The pathogenicity test was conducted as described by Wei, Huang, Gao, Ke, and Kang (2010). Leaves were washed with tap water, immersed in 0.6% sodium hypochlorite for 3 min and then rinsed three times with sterile water. Moistened cotton was wrapped around the basal parts of the petioles to keep them wet. Four small wounds were made on each leaf using a sterile needle. The wounds were inoculated by placing a 5-mm-diameter PDA culture block onto each of the four wounds. The leaves were placed in a plastic box, which was immediately covered with vinyl film to retain the humidity, and incubated in the dark at 25°C. The twigs used in the pathogenicity assays were washed with

tap water, immersed in 1% sodium hypochlorite for 10 min and then rinsed three times with sterile water. The top end of each twig was sealed with wax before inserting the end in sand in a plastic basin. Each twig segment was wounded using a flat iron (5-mm-diameter), and then inoculated by placing a 5-mm PDA culture block onto each wound. Then, the basin was immediately covered with vinyl film to retain the humidity and incubated in the dark at 25°C. The lesion diameters were measured, and the statistical significance of differences was determined as described above. Three replicates of the infection assays were performed with six leaves/twigs in each replicate.

2.7 | RNA isolation, cDNA synthesis and qRT-PCR

Apple tissue infected with the WT strain was sampled at 0 and 24 hpi (hours post-inoculation). The total RNA of each sample was extracted using Trizol Reagent (Invitrogen, Carlsbad, CA) according to the manufacturer's instructions, and DNA contamination was prevented by DNase I treatment. First-strand cDNA was synthesized using an RT-PCR system (Promega, Madison, WI, USA) according to the manufacturer's instructions. Quantitative PCR amplifications were performed using a CFX96 Real-Time System (Bio-Rad) with SYBR Green I chemistry (Invitrogen). The *V. mali* housekeeping gene *G6PDH* was used as an internal reference control to determine the relative gene expression levels of *VMAGO2* (Yin et al., 2013). The relative expression level of *VMAGO2* was calculated as the fold change in inoculated plants versus mock-inoculated plants at the same time point using the comparative 2^{- $\Delta\Delta$ CT} method (Livak & Schmittgen, 2001). Three biological replicates were performed for each experiment. The primers used are listed in Table S1.

2.8 | Generation of the *VMAGO2* complementary strain

The entire *VMAGO2* gene fragment and its whole promoter sequence (~1,500 bp) were amplified from genomic DNA using the primer pairs *VMAGO2*-CM-F/R (Table S1) and cloned into pFL2 using the yeast gap repair approach, as described by Zhou, Li, and Xu (2011). Fusion constructs were confirmed by sequencing, and plasmids were transformed into the corresponding deletion mutants by PEG-mediated transformation (Gao et al., 2011). The transformants were confirmed by PCR. The phenotype of the complementary strains was determined using the methods described above.

3 | RESULTS

3.1 | Protein sequence and phylogenetic tree analysis

Based on the genome information of *V. mali*, the *VMAGO2* gene sequence was obtained. InterProScan analyses showed that the deduced *VMAGO2* protein contained three domains, known as DUF1785 (a domain usually found in Argonaute proteins that often co-occurs with the PIWI domain), PZA (an evolutionarily conserved

domain of Argonaute proteins, whose primary function is to bind the 3' end of small RNAs) and PIWI (a domain found in the Argonaute family of related proteins, whose function is double-stranded-RNA-guided hydrolysis of single-stranded RNA) (Figure 1a). As expected, the phylogenetic analysis suggested that the VMAGO2 is clustered with AGOs in fungi and also appears to share a common ancestor with AGOs in plants and animals (Figure 1b).

3.2 | VMAGO2 was upregulated during pathogen infection

To investigate how VMAGO2 is regulated in *V. mali* during the infection process, qRT-PCR was used to analyse its transcript level changes. The analysis showed that VMAGO2 expression was 3.4-fold higher than that of the control (mycelium) at 24 hpi (Figure 2).

3.3 | Construction of VMAGO2 deletion mutants

As shown in Figure 3, the positive deletion mutants were identified and confirmed via screening using PCR and Southern blot hybridization. When we amplified the ORF segment of VMAGO2, no product was amplified using the Δ VMAGO2 mutant DNA (Figure 3b; Lane 1), but the *hph* segment was amplified (Figure 3b; Lane 2). An obvious band could also be seen when the segment was amplified using the primers of VMAGO-1F/H855R and H856F/VMAGO2-4R (Figure 3b; Lanes 3 and 4). All putative knockout mutants were further verified by Southern blot hybridization. When hybridized with an *hph* probe, no hybridization signal was observed for the WT strain and a 4.0 kb *Xho* I band was observed for the Δ VMAGO2 mutant. When hybridized with a VMAGO2 fragment, a 4.5 kb *Pst* I band was observed for the WT, while no corresponding hybridization signal was observed for the Δ VMAGO2 mutant (Figure 3c). These results indicated that we generated six positive VMAGO2 knockout mutants.

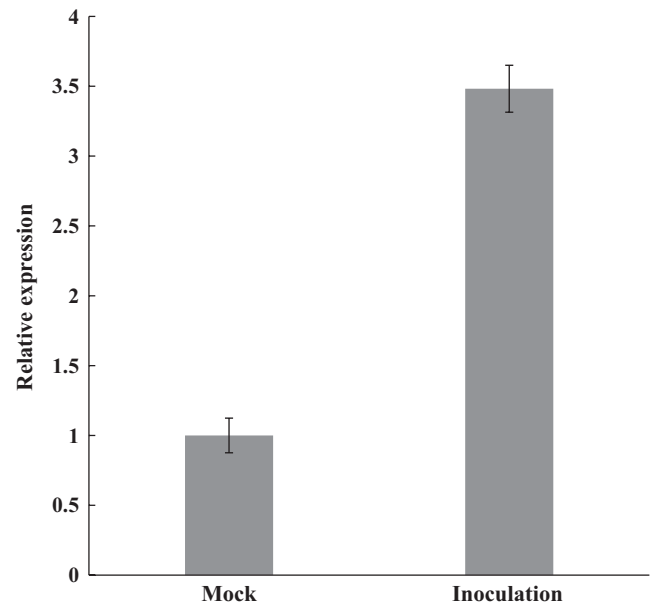


FIGURE 2 The relative expression of VMAGO2 during the infection process of *Valsa mali*. The expression profile of VMAGO2 at 24 hpi (hours post-inoculation) compared with that of the control (mycelium) using reference gene *G6PDH* for normalization. Vertical bars represent the standard deviations of the means of three independent replicates

3.4 | VMAGO2 is not essential for *Valsa mali* vegetative growth

To investigate whether VMAGO2 plays a critical role in the growth and development of *V. mali*, the growth rate and the colony and hyphal morphology of the mutants (Δ VMAGO2 and Δ VMAGO2-C) and WT were compared. The colonial morphologies of the mutant and WT strains were not obviously different, and the growth rate of

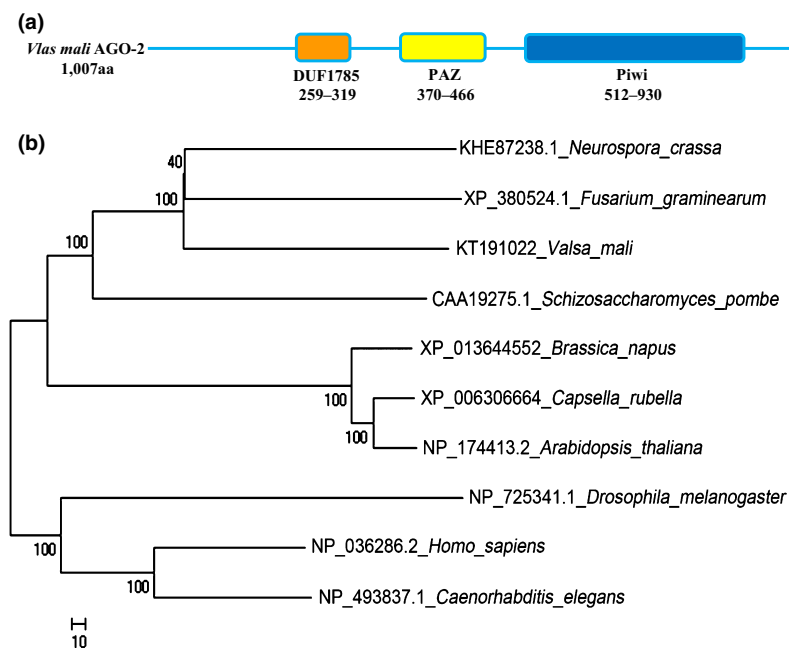


FIGURE 1 Domains and homologous analysis of the VMAGO2 protein. (a) The deduced VMAGO2 protein contains three domains, DUF1785, PAZ and PIWI, which were predicted at the 259–319, 370–466 and 512–930 amino acid sites, respectively. (b) A phylogenetic tree of VMAGO2 proteins constructed with the multiple alignment program DNAMAN using the AGO protein sequences from plants, animals and fungi. VMAGO2 proteins were clustered with AGOs from fungi and shared a common ancestor with AGOs in plants and animals. The GenBank accession numbers and the species names of the organisms within the clade are shown

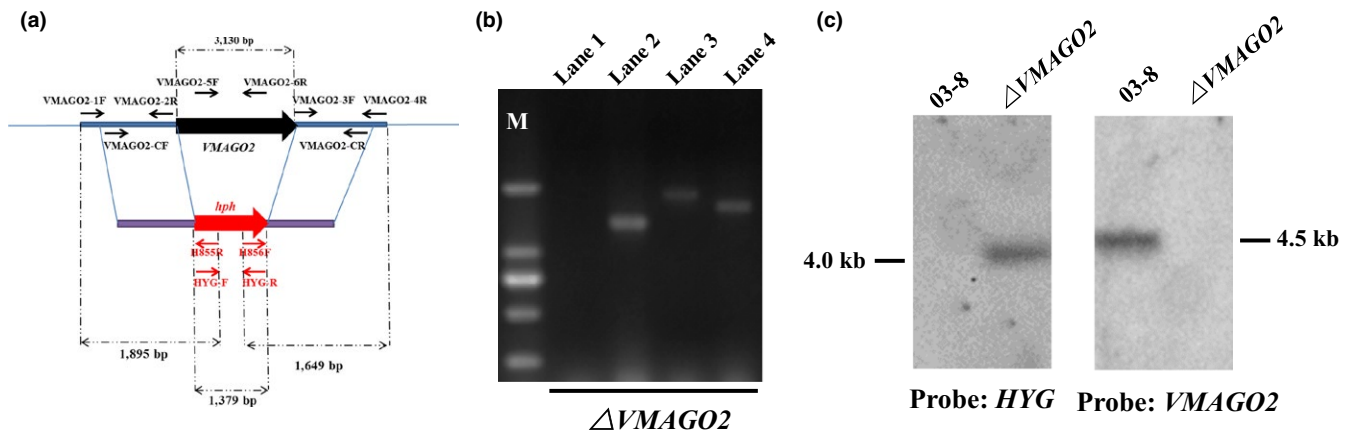


FIGURE 3 Construction of $\Delta VMAGO2$ mutants. (a) A physical map of the *VMAGO2* genomic region and gene replacement constructs. (b) PCR detection of $\Delta VMAGO2$ using four pairs of primers. M: DL2000. Lane 1: product amplified by 5F/6R to detect the *VMAGO2*. Lane 2: product amplified by H852/H850 to detect the insertion of *HYG*. Lane 3 and lane 4: products amplified by 1F/H855R and H856F/4R, which were used to ensure homologous recombination upstream and downstream, respectively. (c) Southern blot detection of $\Delta VMAGO2$. Genomic DNA of WT and $\Delta VMAGO2$ strains was isolated and digested with the restriction enzymes *Xho I* and *Pst I*, respectively. The DNA was hybridized with *HYG* probes and *VMAGO2* fragments with 4.0 and 4.5 kb bands, respectively

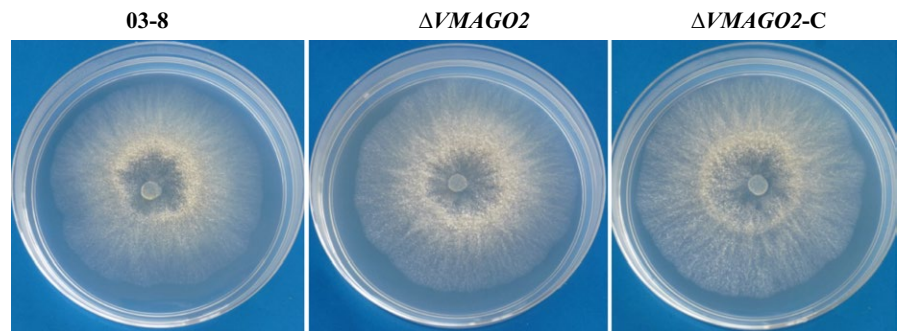


FIGURE 4 Colonial morphology of mutants and wild-type (WT). Two-day-old WT, $\Delta VMAGO2$ and $\Delta VMAGO2-C$ cultures growing on potato dextrose agar (PDA) medium at 25°C in the dark

$\Delta VMAGO2$ and WT were 2.662 cm/day and 2.591 cm/day, respectively (Figure 4). All six positive mutants exhibited a similar phenotype (detailed data not shown).

3.5 | Deletion of *VMAGO2* increases the sensitivity of *Valsa mali* to 0.05% H_2O_2

The response of the *VMAGO2* mutants and WT to osmotic stresses was also evaluated. After 7 days incubation at 25°C, we found that the growth of $\Delta VMAGO2$ and WT was severely restricted under the treatment conditions and that the colony diameters were similar (Figure 5a). The response of the $\Delta VMAGO2$ mutant to different pH levels (pH 2–11) was also examined. After incubation for 2 days, both the $\Delta VMAGO2$ mutant and WT exhibited normal growth under acid conditions, but neither of them showed normal growth under alkaline conditions. In general, knockout of the *VMAGO2* did not result in an altered response to pH when compared to the WT response (Figure 5b). The response of *VMAGO2* mutants to oxidative stress was also evaluated. In the presence of 0.05% H_2O_2 , vegetative growth of $\Delta VMAGO2$ was severely restricted (the mutant showed almost no growth), while the complementary strain showed normal growth when compared with that of the WT (Figure 6a,b). These results suggested that *VMAGO2* may be important for oxidative stress responses.

3.6 | The *VMAGO2* gene is critical for pathogen virulence on apple leaves and twigs

To test whether the *VMAGO2* mutants showed similar virulence defects, a pathogenicity assay was performed using apple leaves and twigs of “Fuji.” The infection assay results showed that $\Delta VMAGO2$ was significantly less virulent on both leaves and twigs than the WT strain (Figure 7a,b). Furthermore, the average lesion diameter on leaves and twigs inoculated with the $\Delta VMAGO2$ strain was 34.8% and 19.8% smaller, respectively, than the lesions caused by the WT strain (Figure 7c,d). The compromised pathogenicity could be recovered by complementation of the $\Delta VMAGO2$ mutants with *VMAGO2*. These results suggested that *VMAGO2* plays a positive role during the *V. mali* infection process. Unravelling the detailed mechanism will be a key aim of future studies.

4 | DISCUSSION

Argonaute proteins are ubiquitous in plants and animals, common in many fungi and protists, and present in some archaea (Pratt & MacRae, 2009). In this study, we identified *VMAGO2* in *V. mali*. *VMAGO2* has domains that are typical of AGO proteins. Evolutionary

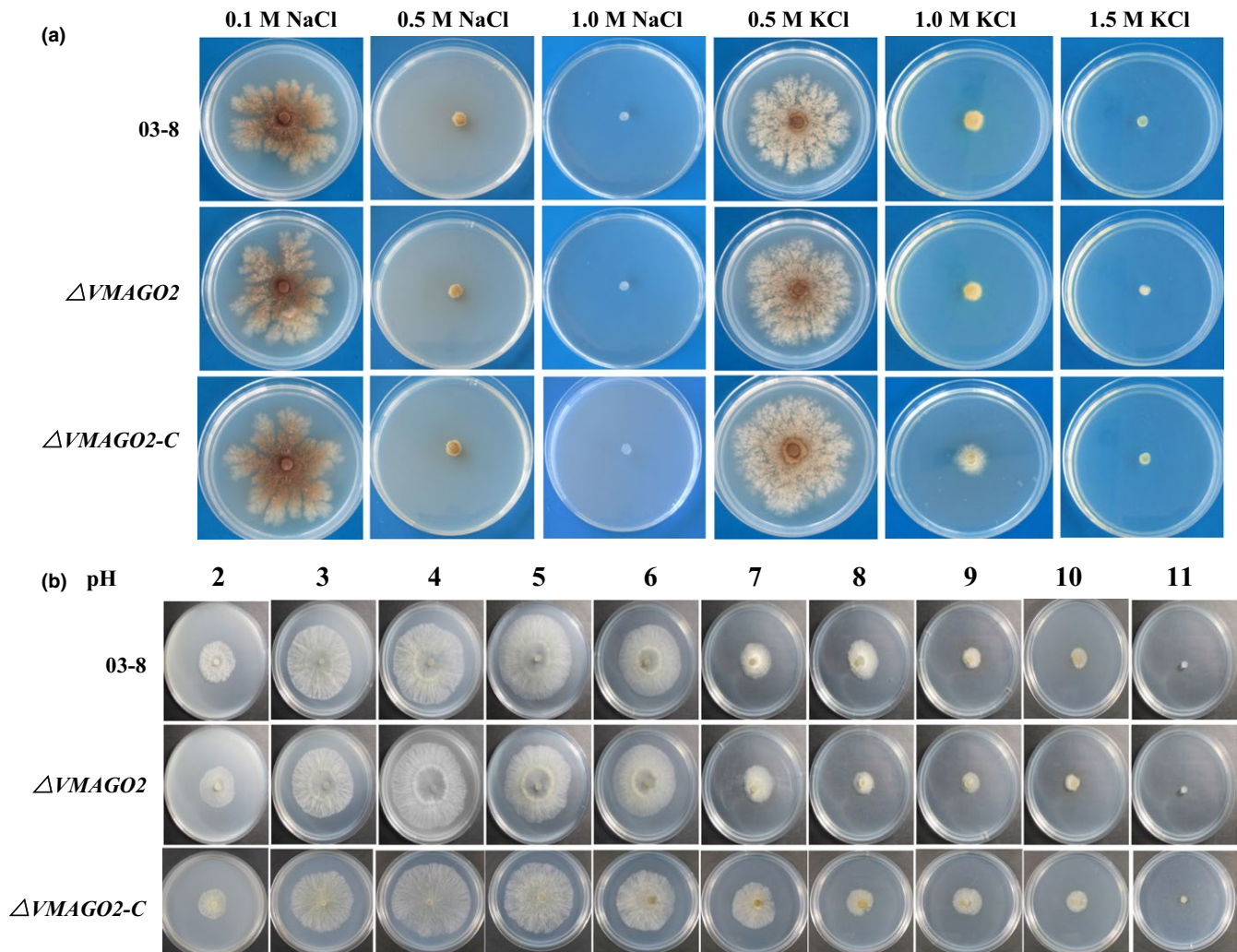


FIGURE 5 Responses of mutants and wild-type (WT) to osmotic stresses and different pH values. (a) Seven-day-old cultures of WT and $\Delta VMAGO2$ growing on potato dextrose agar (PDA) media supplemented with 0.1, 0.5 or 1.0 M NaCl or with 0.5, 1.0 or 1.5 M KCl at 25°C in the dark. (b) Two-day-old cultures of WT and $\Delta VMAGO2$ growing on PDA media with pH values ranging from 2 to 11 at 25°C in the dark

tree analysis revealed that *VMAGO2* is closely homologous to fungal AGOs. Indeed, the sRNA pathways appear to be relatively conserved in fungi, and the AGO proteins have been identified in several fungi, particularly in ascomycetes (Nunes et al., 2011).

Previous studies have shown that disruptions of AGOs can affect the vegetative growth and responses to environmental signals of *M. circinelloides* and *Colletotrichum higginsianum* (Campo, Gilbert, & Carrington, 2016; Cervantes et al., 2013). In our study, when *VMAGO2* was knocked out, the colony morphology of the mutants, and their responses to saline ion stresses and different pHs were not significantly different to those of the WT. One possible explanation for this is that the functions of *VMAGO* genes are redundant. A previous study has shown that the *Caenorhabditis elegans* AGO proteins ALG-1 and ALG-2 have overlapping functions (Grishok et al., 2001). Indeed, different AGOs belonging to the same gene family can have special and unique functions. For example, of the four AGO proteins in humans, only AGO2 is a catalytically active slicer (Liu et al., 2004).

As plant pathologists, our main interest in this study was the pathogenicity contributed by *VMAGO2*. An accumulation of hydrogen peroxide in host plant tissues is considered to be an early sign of a plant–pathogen interaction (Bolwell, 1999). Hydrogen peroxide not only works as a signal to activate the resistance reactions of the plant, but also kills pathogens directly when it has accumulated to a certain level (Torres, Jones, & Dangl, 2006). In this study, we found that the expression of *VMAGO2* was highly induced during the *V. mali* infection process. More importantly, $\Delta VMAGO2$ showed a greater sensitivity to hydrogen peroxide stress and a significantly decreased pathogenicity compared with *VMAGO2*. Further investigations are needed to determine whether the decreased pathogenicity is related with the increased sensitivity to hydrogen peroxide.

During the interaction between the pathogen and the host plant, sRNAs play pivotal roles by regulating the corresponding target genes. The RNAi pathway has been shown to play an important role in the plant response to pathogen infection (Huang, Yang, & Zhang, 2016; Voinnet, 2008). A recent study reported that fungal

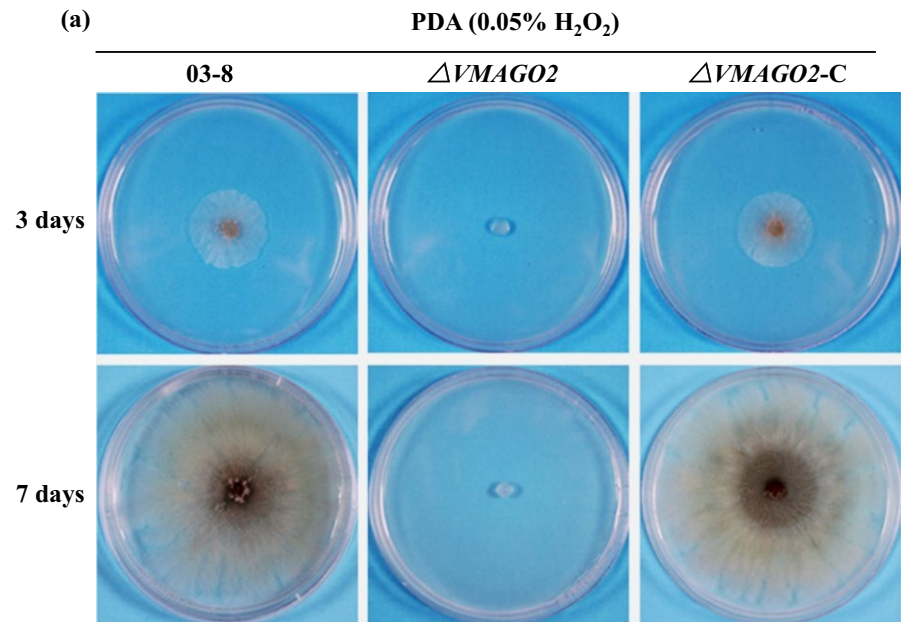


FIGURE 6 Defects of mutants and wild-type (WT) response to hydrogen peroxide stress. (a) Three- and seven-day-old cultures of WT, $\Delta VMAGO2$ and $\Delta VMAGO2-C$ growing on potato dextrose agar (PDA) medium containing 0.05% H₂O₂ at 25°C in the dark. (b) Colony diameter of the WT, $\Delta VMAGO2$ and $\Delta VMAGO2-C$. The diameter of the colony was determined using the crossing method. The Bars indicate the standard deviation of the mean of three replicates. The stars above the bars indicate significantly different means (least significant difference [LSD] test, $p < .05$)

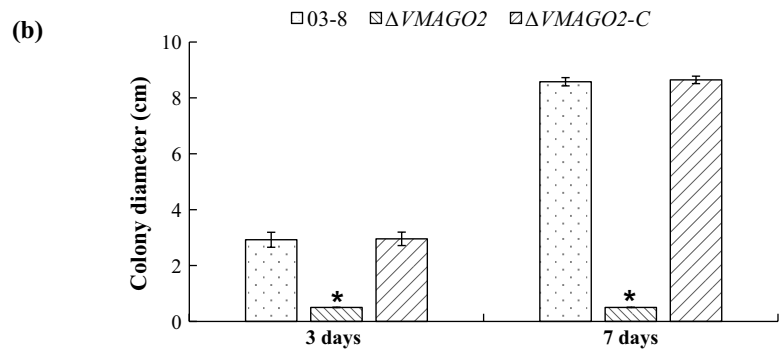
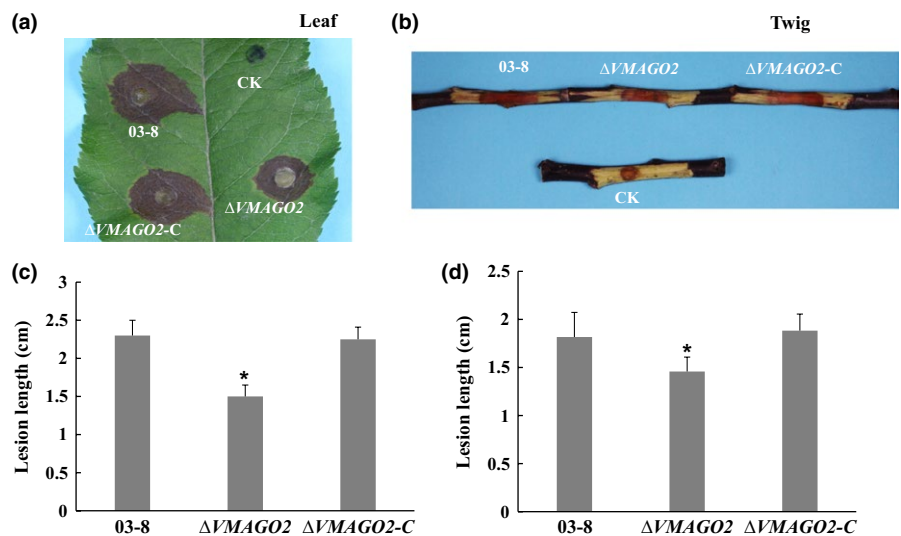


FIGURE 7 Pathogenicity of mutants and wild-type (WT). (a and b) “Fuji” apple (*Malus domestica* cv “Fuji”) leaves and twigs showing the pathogenicity of the mutants relative to the WT. The control leaves and twigs (CK) were inoculated with sterile potato dextrose agar (PDA) blocks. (c and d) The lesion diameter of apple leaves and twigs 3 days after inoculation. The bar indicates the standard deviation of the mean of three replicates. The stars above the bars indicate significantly different means (least significant difference [LSD] test, $p < .05$). The infection assays were repeated eight times with three biological replicates



sRNAs were able to affect the host RNAi pathways by targeting the host AGO genes, which suppressed the plant immune response (Ellendorff et al., 2009; Weiberg et al., 2013). In fungi, the generation of sRNAs is complex and varies in different species (Nicolás & Ruiz-Vázquez, 2013). AGOs may also be involved in the generation of sRNAs (Lee et al., 2009). Although it has not been confirmed

whether an AGO protein could perform its biological functions by interacting with other proteins as a common coding protein, the main role of AGO proteins is to combine sRNAs. Thus, in further studies, we will isolate the sRNAs combined by VMAGO2, and explore the molecular functions of VMAGO2 in the regulatory mechanisms of sRNAs.

In summary, the *V. mali* AGO2 gene was identified, and characterization of its biological functions indicates roles related to the hydrogen peroxide stress response and the pathogenicity of *V. mali*. Our results provide an insight into the roles of VMAGO2 in *V. mali*, especially the regulation of pathogenicity by *V. mali* sRNAs.

ACKNOWLEDGEMENTS

We thank Dr Fengming Song for providing the gene deletion vector. This work was financially supported by the National Natural Science Foundation of China (No. 31501591), The China Postdoctoral Science Foundation Special Funding (2016T90953) and the Doctoral Scientific Research Foundation of Northwest A&F University.

REFERENCES

- Agorio, A., & Vera, P. (2007). ARGONAUTE4 is required for resistance to *Pseudomonas syringae* in *Arabidopsis*. *Plant Cell*, *19*, 3778–3790.
- Agrawal, N., Dasaradhi, P. V., Mohammed, A., Malhotra, P., Bhatnagar, R. K., & Mukherjee, S. K. (2003). RNA interference: Biology, mechanism, and applications. *Microbiology and Molecular Biology Reviews*, *67*, 657–685.
- Bartel, D. P. (2004). MicroRNAs: Genomics, biogenesis, mechanism, and function. *Cell*, *116*, 281–297.
- Bolwell, G. P. (1999). Role of active oxygen species and NO in plant defence responses. *Current Opinion in Plant Biology*, *2*, 287–294.
- Campo, S., Gilbert, K. B., & Carrington, J. C. (2016). Small RNA-based antiviral defense in the phytopathogenic fungus *Colletotrichum higginsianum*. *PLoS Pathogens*, *12*, e1005640.
- Cao, K., Guo, L., Li, B., Sun, G., & Chen, H. (2009). Investigations on the occurrence and control of apple canker in China. *Plant Protection*, *35*, 114–116 (in Chinese).
- Cervantes, M., Vila, A., Nicolás, F. E., Moxon, S., de Haro, J. P., Dalmay, T., ... Ruiz-Vázquez, R. M. (2013). A single argonaute gene participates in exogenous and endogenous RNAi and controls cellular functions in the basal fungus *Mucor circinelloides*. *PLoS One*, *8*, e69283.
- Duan, C. G., Fang, Y. Y., & Zhou, B. J. (2012). Suppression of *Arabidopsis* ARGONAUTE1-mediated slicing, transgene-induced RNA silencing, and DNA methylation by distinct domains of the cucumber mosaic virus 2b protein. *Plant Cell*, *24*, 259–274.
- Ellendorff, U., Fradin, E. F., de Jonge, R., & Thomma, B. P. (2009). RNA silencing is required for *Arabidopsis* defence against *Verticillium* wilt disease. *Journal of Experimental Botany*, *60*, 591–602.
- Gao, J., Li, Y., Ke, X., Kang, Z., & Huang, L. (2011). Development of genetic transformation system of *Valsa mali* of apple mediated by PEG. *Acta Microbiologica Sinica*, *51*, 1194–1199 (in Chinese).
- Grishok, A., Pasquinelli, A. E., Conte, D., Li, N., Parrish, S., Ha, I., ... Mello, C. C. (2001). Genes and mechanisms related to RNA interference regulate expression of the small temporal RNAs that control *C. elegans* developmental timing. *Cell*, *106*, 23–34.
- Hu, Y., Stenlid, J., Elfstrand, M., & Olson, A. (2013). Evolution of RNA interference proteins dicer and argonaute in *Basidiomycota*. *Mycologia*, *105*, 1489–1498.
- Huang, J., Yang, M., & Zhang, X. (2016). The function of small RNAs in plant biotic stress response. *Journal of Integrative Plant Biology*, *58*, 312–327.
- Hutvagner, G., & Simard, M. J. (2008). Argonaute proteins: Key players in RNA silencing. *Nature Reviews Molecular Cell Biology*, *9*, 22–32.
- Jinek, M., & Doudna, J. A. (2009). A three-dimensional view of the molecular machinery of RNA interference. *Nature*, *457*, 405–412.
- Jöchl, C., Rederstorff, M., Hertel, J., Stadler, P. F., Hofacker, I. L., Schrettl, M., ... Hüttenhofer, A. (2008). Small ncRNA transcriptome analysis from *Aspergillus fumigatus* suggests a novel mechanism for regulation of protein synthesis. *Nucleic Acids Research*, *36*, 2677–2689.
- Joshua-Tor, L. (2004). siRNA sat RISC. *Structure*, *12*, 1120–1122.
- Ke, X., Yin, Z., Song, N., Dai, Q., Voegelé, R. T., Liu, Y., ... Huang, L. (2014). Transcriptome profiling to identify genes involved in pathogenicity of *Valsa mali* on apple tree. *Fungal Genetics and Biology*, *68*, 31–38.
- Kim, Y. K., Heo, I., & Kim, V. N. (2010). Modifications of small RNAs and their associated proteins. *Cell*, *143*, 703–709.
- Lee, H. C., Chang, S. S., Choudhary, S., Aalto, A. P., Maiti, M., Bamford, D. H., & Liu, Y. (2009). qiRNA, a new type of small interfering RNA induced by DNA damage. *Nature*, *459*, 274–277.
- Lee, D. W., Pratt, R. J., McLaughlin, M., & Aramayo, R. (2003). An argonaute-like protein is required for meiotic silencing. *Genetics*, *164*, 821–828.
- Li, Z., Yin, Z., Fan, Y., Xu, M., Kang, Z., & Huang, L. (2015). Candidate effector proteins of the necrotrophic apple canker pathogen *Valsa mali* can suppress BAX-induced PCD. *Frontiers in Plant Science*, *6*, 579.
- Liu, J., Carmell, M. A., Rivas, F. V., Marsden, C. G., Thomson, J. M., Song, J. J., ... Hannon, G. J. (2004). Argonaute2 is the catalytic engine of mammalian RNAi. *Science*, *305*, 1437–1441.
- Livak, K. J., & Schmittgen, T. D. (2001). Analysis of relative gene expression data using real-time quantitative PCR and the $2^{-\Delta\Delta CT}$ method. *Methods*, *25*, 402–408.
- Mallory, A., & Vaucheret, H. (2010). Form, function, and regulation of ARGONAUTE proteins. *Plant Cell*, *22*, 3879–3889.
- Möller, E. M., Bahnweg, G., Sandermann, H., & Geiger, H. H. (1992). A simple and efficient protocol for isolation of high molecular weight DNA from filamentous fungi, fruit bodies, and infected plant tissues. *Nucleic Acids Research*, *20*, 6115–6116.
- Nicolás, F. E., & Ruiz-Vázquez, R. M. (2013). Functional diversity of RNAi-associated sRNAs in fungi. *International Journal of Molecular Sciences*, *14*, 15348–15360.
- Nunes, C. C., Sailsbery, J. K., & Dean, R. A. (2011). Characterization and application of small RNAs and RNA silencing mechanisms in fungi. *Fungal Biology Reviews*, *25*, 172–180.
- Okamura, K., Ishizuka, A., & Siomi, H. (2004). Distinct roles for Argonaute proteins in small RNA-directed RNA cleavage pathways. *Genes & Development*, *18*, 1655–1666.
- Pratt, A. J., & MacRae, I. J. (2009). The RNA-induced silencing complex: A versatile gene-silencing machine. *Journal of Biological Chemistry*, *287*, 17897–17901.
- Sun, Q., Choi, G. H., & Nuss, D. L. (2009). A single Argonaute gene is required for induction of RNA silencing antiviral defense and promotes viral RNA recombination. *Proceedings of the National Academy of Sciences of the United States of America*, *106*, 17927–17932.
- Torres, M. A., Jones, J. D. G., & Dangl, J. L. (2006). Reactive oxygen species signaling in response to pathogens. *Plant Physiology*, *141*, 373–378.
- Voinnet, O. (2008). Post-transcriptional RNA silencing in plant-microbe interactions: A touch of robustness and versatility. *Current Opinion in Plant Biology*, *11*, 464–470.
- Wang, X., Zang, R., Yin, Z., Kang, Z., & Huang, L. (2014). Delimiting cryptic pathogen species causing apple *Valsa* canker with multilocus data. *Ecology and Evolution*, *4*, 1369–1380.
- Wei, J., Huang, L., Gao, Z., Ke, X., & Kang, Z. (2010). Laboratory evaluation methods of apple *Valsa* canker disease caused by *Valsa ceratosperma* sensu Kobayashi. *Acta Phytopathologica Sinica*, *40*, 14–20 (in Chinese).
- Weiberg, A., Wang, M., Lin, F. M., Zhao, H., Zhang, Z., Kaloshian, I., ... Jin, H. (2013). Fungal small RNAs suppress plant immunity by hijacking host RNA interference pathways. *Science*, *342*, 118–123.
- Yin, Z., Ke, X., Huang, D., Gao, X., Voegelé, R. T., Kang, Z., & Huang, L. (2013). Validation of reference genes for gene expression analysis in *Valsa mali* var. *mali* using real-time quantitative PCR. *World Journal of Microbiology and Biotechnology*, *29*, 1563–1571.

- Yin, Z., Liu, H., Li, Z., Ke, X., Dou, D., Gao, X., ... Huang, L. (2015). Genome sequence of *Valsa* canker pathogens uncovers a potential adaptation of colonization of woody bark. *New Phytologist*, 208, 1202–1216.
- Yin, Z., Zhu, B., Feng, H., & Huang, L. (2016). Horizontal gene transfer drives adaptive colonization of apple trees by the fungal pathogen *Valsa mali*. *Scientific Reports*, 6, 33129.
- Yu, J. H., Hamari, Z., Han, K. H., Seo, J. A., Reyes-Domínguez, Y., & Scazzocchio, C. (2004). Double-joint PCR: A PCR-based molecular tool for gene manipulations in filamentous fungi. *Fungal Genetics and Biology*, 41, 973–981.
- Yuan, Y. R., Pei, Y., Ma, J. B., Kuryavyi, V., Zhadina, M., Meister, G., ... Patel, D. J. (2005). Crystal structure of *A. aeolicus* argonaute, a site-specific DNA-guided endoribonuclease, provides insights into RISC-mediated mRNA cleavage. *Molecular Cell*, 19, 405–419.
- Zhou, X., Li, G., & Xu, J. R. (2011). Efficient approaches for generating GFP fusion and epitope-tagging constructs in filamentous fungi. In J.-R. Xu

& B. H. Bluhm (Eds.), *Fungal genomics: Methods and protocols* (pp. 199–212). New York, NY: Humana Press, Springer Verlag.

SUPPORTING INFORMATION

Additional Supporting Information may be found online in the supporting information tab for this article.

How to cite this article: Feng H, Xu M, Liu Y, et al. The distinct roles of Argonaute protein 2 in the growth, stress responses and pathogenicity of the apple tree canker pathogen. *For Path.* 2017;00:e12354. <https://doi.org/10.1111/efp.12354>